Applied Thermal Engineering 110 (2017) 1091–1100

Contents lists available at ScienceDirect

Applied Thermal Engineering

journal homepage: www.elsevier.com/locate/apthermeng

A comparative study on the performance of HFO-1234yf and HFC-134a as an alternative in automotive air conditioning systems

Samaneh Daviran [a], Alibakhsh Kasaeian [a,*], Soudabeh Golzari [a], Omid Mahian [b], Shahin Nasirivatan [c], Somchai Wongwises [d,*]

[a] Department of Renewable Energies, Faculty of New Science & Technologies, University of Tehran, Tehran, Iran
[b] Young Researchers and Elite Club, Mashhad Branch, Islamic Azad University, Mashhad, Iran
[c] Faculty of Mechanical Engineering, Sharif University of Technology, Tehran, Iran
[d] Fluid Mechanics, Thermal Engineering and Multiphase Flow Research Lab. (FUTURE), Department of Mechanical Engineering, Faculty of Engineering, King Mongkut's University of Technology Thonburi, Bangmod, Bangkok, Thailand

HIGHLIGHTS

- Performance of automotive an air conditioning system by two refrigerants is studied.
- Compressor work for HFO-1234yf refrigerant is higher than HFC-134a refrigerant.
- The discharge temperature of compressor and pressure ratio of HFO-1234yf is lower.
- In constant mass flow rates, COP of HFO-1234yf is 18% higher than that of HFC-134a.

ARTICLE INFO

Article history:
Received 24 April 2016
Revised 3 September 2016
Accepted 7 September 2016
Available online 9 September 2016

Keywords:
Air conditioning
COP
Simulation
Refrigerant
GWP

ABSTRACT

In this study, an automotive air conditioning system is simulated by considering HFO-1234yf (2,3,3,3-tetrafluoropropene) as the drop-in replacement of HFC-134a. The simulated air conditioning system consists of a multi-louvered fin and flat-plate type evaporator, a wobble-plate type compressor, a mini-channel parallel-flow type condenser and a thermostatic expansion valve. The thermodynamic properties of the refrigerants are extracted from the REFPROP 8.0 software, and a computer program is simulated for the thermodynamic analysis. Two different conditions have been considered in this program for the cycle analysis: for the first state, the cooling capacity is taken as constant, and for the second state the refrigerant mass flow rate is considered fixed. The performance characteristics of system including COP and cooling capacity have been studied with changing different parameters. The results show that the refrigerant-side overall heat transfer coefficient of HFO-1234yf is 18–21% lower than that of HFC-134a, and the pressure drop is 24% and 20% smaller than HFC-134a during condensing and evaporating processes, respectively. Also, in a constant cooling capacity, the COP of HFO-1234yf is lower than HFC-134a by 1.3–5%, and in the second case the COP of HFO-1234yf is about 18% higher than that of HFC-134a.

1. Introduction

The matter of ozone depletion potential (ODP) of chlorofluorocarbon (CFC) and hydrochlorofluorocarbon (HCFC) refrigerants caused the use of hydrofluorocarbon (HFC) refrigerants to increase progressively over the last 20 or so years. Many of the HFC refrigerants have relatively large values of global warming potential although they have no ozone depletion potential. They are one of the six greenhouse gases and their emission must be decreased according to the Kyoto Protocol (1997). Many researchers have tried to find alternative refrigerants to conventional HFCs. The European Union's f-gas regulations (Regulation (EC) No 842/2006 and Directive 2006/40/EC) instituted a gradual ban on fluorinated greenhouse gases. The manufacturing of new models was prohibited on January 1, 2011, and producing new models and new vehicles with air-conditioning containing fluorinated greenhouse gases having global warming potentials (GWP) greater than 150 [1] will be prohibited on January 1, 2017.

Brown et al. [2] evaluated the performance of CO2 and HFC-134a in a semi-theoretical cycle and reported a higher COP for HFC-134a compared to the CO2. According to the model presented by Joudi et al. [3], a mixture of R290/R600 could be the best

* Corresponding authors.
E-mail addresses: [redacted]@gmail.com (A. Kasaeian), [redacted]@kmutt.ac.th (S. Wongwises).

http://dx.doi.org/10.1016/j.applthermaleng.2016.09.034
1359-4311/

Nomenclature

A_0	total air-side surface area [m^2]
A_c	minimum free flow area for air-side [m^2]
A_f	fin surface are [m^2]
ALT	atmospheric life time
COP	coefficient of performance
f	fanning friction factor
F_h	fin height [mm]
F_p	fin pitch [mm]
GWP	global warming potential
G	refrigerant mass flux [$kg\ m^{-2}\ s^{-1}$]
h	specific enthalpy [$kJ\ kg^{-1}$] or heat transfer coefficient [$W\ m^{-2}\ K^{-1}$]
j	Colburn j factor, $Nu/(Re\ Pr^{1/3})$
L_a	louver angle
L_d	fin length [mm]
L_h	louver height [mm]
L_p	louver pitch [mm]
LCCP	life cycle climate performance
LMTD	logarithmic mean temperature difference
m	mass flow rate [$kg\ s^{-1}$]
n	rotational speed of compressor [rpm]
ODP	ozone depletion potential
P	pressure [kpa]
Pr	Prandtl number
Q	heat transfer rate of refrigeration capacity
Re_{Lp}	air-side Reynolds number based on louvered pitch
r	pressure ratio
s	specific entropy [$kJ\ kg^{-1}\ K^{-1}$]
T	temperature [K or °C]
u	velocity [$m\ s^{-1}$]
UA	overall heat transfer coefficient [$W\ K^{-1}$]
VD	Volumetric Displacement [$cc\ s^{-1}$]
W_{comp}	compressor power [kW]
x	quality

Greek symbols

Γ	property index
δ_f	fin thickness [mm]
η_f	fin efficiency
η_s	isentropic efficiency of compressor
η_v	volumetric efficiency of compressor
μ	dynamic viscosity [Pa s]
ν	kinematic viscosity [$m^2\ s^{-1}$]
ρ	density [$kg\ m^{-3}$]
σ	surface tension [$N\ m^{-1}$]

Subscripts

a	air
c	condenser
e	evaporator
i	in
o	out
r	refrigerant
sh	superheat region
sc	subcooled region
lo	liquid only

alternative for R12. Hydrocarbons, neglecting their flammability, have a high potential for making high COP. The experimental results of Wongwise et al. [4] for a mixture of propane/*n*-butane/isobutene with a molar ratio of 50/40/10 show a better performance compared to HFC-134a. Another experimental investigation states that the COP of R290/R600a may be better than the COP of R12 and HFC-134a [5]. An algorithm has been presented by Arcaklioğlu et al. [6] for finding mixtures of refrigerants that would have the same volumetric cooling capacity (VCC) as CFCs in the compression refrigeration systems. The Dupont and Honeywell companies presented some information about a new refrigerant in the European Workshop on Mobile Air Conditioning & Auxiliaries in Torino, Italy. This new refrigerant is a hydrofluro olefin, like 2,3,3,3 tetrafluropropene, which is named HFO-1234yf [7]. This refrigerant has a similar thermophysical property to what HFC-134a has, and hence there is no necessity for a significant change on the equipment. The mentioned refrigerant has achieved the proper stability (chemical & thermal) and compatibility values, has no observable corrosion effects on metals, and its environmental properties are desired (ODP = 0, GWP = 4, ALT = 11 days and also proper LCCP) [8]. Brown et al. [9] carried out research on a replacement of R114 by HFO-1234yf. Their results show that HFO-1234yf has obtained a higher amount of volumetric heat capacity and COP. Also, in the later research, which was done by Zilio et al. [10] on a small-size European car in 2009, no significant decrease in COP and cooling capacity of HFO-1234yf was observed compared to that of HFC-134a. Recently, Zhang et al. [11] theoretically investigated the non-azeotropic mixtures of HFOs (HFO-1234yf, HFO-1234ze(z), HFO-1234ze(e) and HFO-1234zf) as replacements for HFC134a and CFC114 in heat pumps by a simple method. Their results demonstrate that some compositions of these mixtures can have proper COP and may be a better replacement for HCFC134a and CFC114. Some experimental works have been done by Mathur [12] for determination of A/C performance with HFO-1234yf as the working fluid, which was used as a drop-in alternative of HFC-134a. The results demonstrate that the refrigerant mass charge for HFO-1234yf is reduced to 90% of HFC-134a mass charge, cooling capacity and COP are superior to that of HFC-134a and the working pressure of the parallel flow condenser is lower.

Lee and Jung [13] evaluated the performance of HFO-1234yf as a drop-in alternative for HFC-134a under the status of mobile air conditioners in a heat pump testing bench. The tests indicate that the COP of HFO-1234yf is 0.8% to 2.7% lower than that of HFC134a. The discharge temperature of compressor and amount of charge of HFO-1234yf were less than those obtained with HFC134a, about 6.5 °C and 10%.

In the other experimental research, Navarro-Esbrí et al. [14] analyzed HFO-1234yf as a drop-in alternative for HFC-134a in a vapor compression system. The energy performance of HFC-134a and HFO-1234yf was compared under a wide range of working conditions. According to the results, the cooling capacity and COP of HFO-1234yf in an HFC-134a vapor compression system was about 9% and 19% lower than those of HFC-134a. Using an internal heat exchanger notably reduced these differences in the energy performance.

An energy performance assessment of two low-GWP refrigerants, HFO-1234yf and HFO-1234ze(E), as drop-in replacements for HFC134a was experimentally studied by Mota-Babiloni et al. [15]. Tests were performed in a monitored vapor compression system both without and with an internal heat exchanger. Results demonstrated that without an internal heat exchanger the average volumetric efficiency for HFO-1234yf and HFO-1234ze in comparison with HFC-134a was 4% and 5% lower, respectively. Values of

COP for HFO-1234yf and HFO-1234ze are about 7% and 6% lower than HFC-134a as well.

Jankovic et al. [16] presented experimental analyses of HFO-1234yf and HFO-1234ze(E) as drop-in replacements for HFC-134a in a small power refrigeration system. They also develop a simulation model validated with test data. Their analysis was based on two different operating conditions. Results showed that different conclusions could be drawn if the drop-in analysis was carried out in various conditions. In general, HFO-1234yf seems like an adequate drop-in refrigerant for HFC-134a, but HFO-1234ze(E) could perform better when an overridden compressor was used to match the refrigerating system's cooling power.

According to the theoretical and experimental studies mentioned above, there have been just a few theoretical papers in this area and most of the work done with HFO-1234yf was experimental. The purpose of this study is to investigate the theoretically appropriate drop-in replacement of HFC-134a with HFO-1234yf, which is an environmentally friendly refrigerant, by simulating the components of an automotive A/C system.

2. Thermodynamic properties

The thermodynamic properties of the investigated refrigerants were extracted from REFPROP 8.0 Software. The P-h diagram of the two concerned refrigerants, i.e., HFO-1234yf and HFC-134a, are depicted in Fig. 1. According to the diagram, the enthalpies of both refrigerants are nearly identical in the saturated liquid zone, and their difference in the saturated vapor zone is small. It is observed from Table 1 and the previous researches that the thermodynamic characteristics of HFC-134a and HFO-1234yf are close to each other.

3. Simulation of automobile A/C system

For the investigation, an ordinary compression refrigeration cycle is considered. The simulated air conditioning system consists of a multi-louvered fin and flat-plate type evaporator, a wobble-plate type compressor, a mini-channel parallel-flow type condenser and a thermostatic expansion valve, and the presence of a drier is neglected in the simulation. The T-S diagram is shown in Fig. 2, and the schematic of the air conditioning system is presented in Fig. 3.

The performance of HFO-1234yf is simulated as the drop-in replacement of HFC-134a. In the assumed model, the refrigerant enters the evaporator in two phases and exits as superheated vapor. Considering the pressure drop for the refrigerant in the evaporator, the refrigerant temperature decreases in the two-phase region according to Fig. 2.

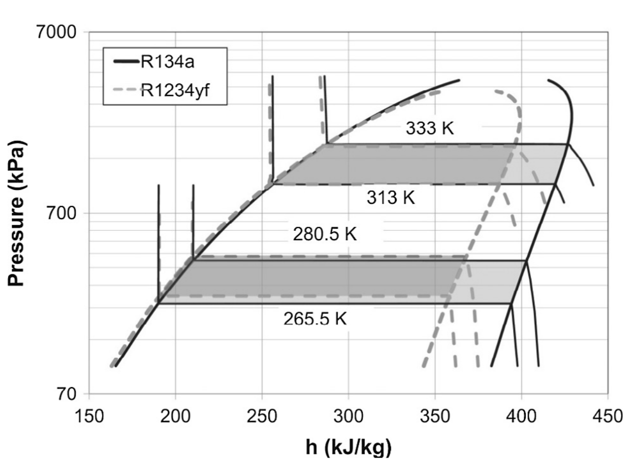

Fig. 1. Log P-h diagram of HFO-1234yf and HFC-134a [14].

Table 1
Thermodynamic properties of HFO-1234yf and HFC-134a (extracted from REFPROP 8.0 Software).

Properties	HFO-1234yf	HFC-134a
Boiling point, T_b [°C]	−29	−26
Critical point, T_c [°C]	95	102
$P_{vap,}$ (25 °C) [MPa]	0.677	0.665
$P_{vap,}$ (80 °C) [MPa]	2.44	2.63
Liquid density, (25 °C) [kg m^{-3}]	1.094	1.207
Vapor density, (25 °C) [kg m^{-3}]	37.6	32.4

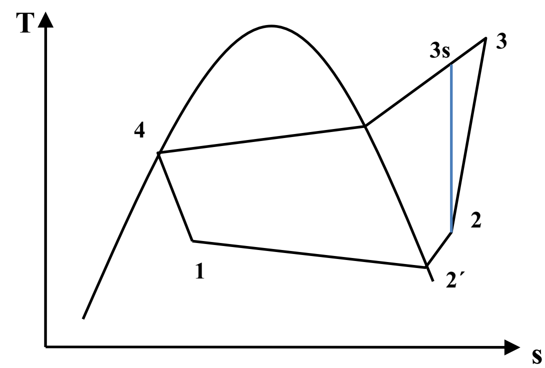

Fig. 2. T-S diagram.

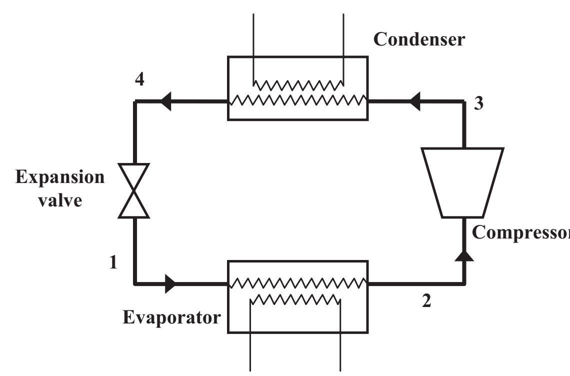

Fig. 3. A schematic of the vapor-compression refrigeration system.

3.1. Heat exchangers model of A/C system

A simulation work was performed to model the thermal performance of HFO-1234yf and HFC-134a as the working fluid to determine the air-side and refrigerant-side heat transfer coefficients and pressure drops. The width of the evaporator was 0.233 m, the height was 0.221 m, and the thickness was 0.038 m. Its outside surface area was 4.2 m^2. The evaporator was divided into a two-phase region and a superheated vapor region. The considered condenser here was a mini-channel parallel flow condenser with 1.56 mm hydraulic diameter channels. Its width was 0.455 m, height was 0.6 m and thickness was 0.02 m. Both evaporator and condenser were taken from SANDEN Co.

For the heat transfer analysis of the heat exchangers, the LMTD method was used. The heat transfer capacities of the heat exchangers were calculated by the inlet and outlet enthalpy difference of the heat exchangers and were remarked as the program checkpoint. The heat transfer formulations were as follows:

$$Q = UA\Delta T_m \tag{1}$$

$$\Delta T_m = \frac{\Delta T_o - \Delta T_i}{\ln\left(\frac{\Delta T_o}{\Delta T_i}\right)} \tag{2}$$

$$Q = m_r(h_o - h_i) \tag{3}$$

The following equation can be used to obtain the overall heat transfer coefficient:

$$\frac{1}{UA} = \frac{1}{h_r A_r} + \frac{\delta_w}{A_w K_w} + \frac{1}{\eta_a h_a A_a} \tag{4}$$

Consider that the second term of the right side of above equation means the tube wall thermal resistance, which has been neglected in this study.

$$\eta_a = 1 - \frac{A_f}{A_a}(1 - \eta_f) \tag{5}$$

$$\eta_f = \sqrt{\frac{\tanh(\acute{m}l)}{(\acute{m}l)}}, \quad \acute{m} = \sqrt{\frac{2h_a}{k_f \delta_f}\left(1 + \frac{\delta_f}{F_d}\right)}, \quad l = \frac{F_h}{2} - \delta_f \tag{6}$$

- Air-side

The pressure loss and heat transfer coefficient of the air-side are written as follows:

$$\Delta P = f\frac{A_o}{A_c}\left(\frac{\rho m V_c^2}{2} - k_c - k_e\right) \tag{7}$$

$$h = \frac{\rho u c_p j}{Pr^{2/3}} \tag{8}$$

where k_c and k_e are the inlet and outlet coefficients of pressure loss of the heat exchangers, respectively. The amounts of k_c and k_e are obtained from the graph given by Kay and London and are 0.4 and 0.2, respectively.

Dong et al. [17] studied the air-side characteristics of multi-louvered fin compact heat exchangers experimentally and presented correlations for the Colburn 'j' factor and Fanning friction 'f' factor as below:

$$f = 0.54486 Re_{Lp}^{-0.3068}\left(\frac{L_a}{90}\right)^{0.444}\left(\frac{F_p}{L_p}\right)^{-0.9925}\left(\frac{F_h}{L_p}\right)^{0.5458}\left(\frac{L_h}{L_p}\right)^{-0.2003}\left(\frac{L_d}{L_p}\right)^{0.0688} \tag{9}$$

$$j = 0.26712 Re_{Lp}^{-0.1944}\left(\frac{L_a}{90}\right)^{0.257}\left(\frac{F_p}{L_p}\right)^{-0.5177}\left(\frac{F_h}{L_p}\right)^{-1.9045}\left(\frac{L_h}{L_p}\right)^{1.7159}\left(\frac{L_d}{L_p}\right)^{-0.2147}\left(\frac{\delta}{L_p}\right)^{-0.05} \tag{10}$$

$$Re_{Lp} = \frac{uL_p}{\vartheta} \tag{11}$$

The geometry of the condenser and evaporator are given in Tables 2 and 3:

- Refrigerant-side

For the calculation of the refrigerant-side heat transfer coefficient, a model has been proposed for single-phase and two-phase by Shah. For the single-phase:

$$h_1 = 0.023\left(\frac{K}{D_h}\right)Re^{0.8}Pr^{0.4} \tag{12}$$

For the two-phase region:

Table 2
The geometry of the condenser (taken from SANDEN CO.).

Width × Height × Depth [mm]	600 × 455 × 20
Fin height [mm]	8
Fin pitch [mm]	1.4
Fin thickness [mm]	0.1
Louver angle [°]	27
Louver pitch [mm]	1.1
Louver length [mm]	7
Flow depth [mm]	24.2
Total tube numbers	35

Table 3
The geometry of the evaporator (taken from SANDEN CO.).

Face area [m^2]	0.051
Refrigerant heat transfer area [m^2]	0.67
Air-side heat transfer area [m^2]	4.2
Number of tubes	24
Tube length [mm]	176.4
Tube thickness [mm]	1.65
Tube pitch [mm]	10.44
Fin height [mm]	8.79
Fin pitch [mm]	1.4
Flow depth	20
Fin thickness [mm]	0.1
Louver angle [°]	30
Louver pitch [mm]	1.3
Louver length [mm]	7

$$h_2 = h_{lo}\left[(1-x)^{0.8} + \frac{3.8x^{0.76}(1-x)^{0.04}}{(P/P_{crit})^{0.04}}\right] \tag{13}$$

where h_{lo} refers to the coefficient of heat transfer with all fluid as liquid. The refrigerant-side heat transfer coefficient is [18]:

$$h_r = \frac{A_1}{A_a}h_1 + \frac{A_2}{A_a}h_2 \tag{14}$$

Neglecting the pressure drop owing to momentum change, a two-phase pressure drop is represented as a pressure drop due to friction [19]:

$$\Delta P_{TP} = \Delta P_{lo}\left[\frac{1}{\Delta x}\int \varphi_{lo}^2 dx\right] \tag{15}$$

where the two-phase multiplier, φ_{lo}, is represented as:

$$\varphi_{lo}^2 = 1 + (4.3\Gamma^2 - 1)[N_{conf}x^{0.875}(1-x)^{0.875} + x^{1.75}] \tag{16}$$

where

$$\Gamma = \left(\frac{\rho_l}{\rho_v}\right)^{0.5}\left(\frac{\mu_v}{\mu_l}\right)^{0.125}, \quad N_{conf} = \frac{1}{d}\left(\frac{\sigma}{g(\rho_l - \rho_v)}\right)^{0.5} \tag{17}$$

3.2. Compressor model

The applied compressor is a wobble-plate type (model: SD7H15 from SANDEN Co.). The compressor power is calculated by the enthalpy difference of refrigerant at entrance and exit:

$$W_{comp} = m_r(h_3 - h_2) \tag{18}$$

The refrigerant mass flow rate may be extracted from the following equation [20]:

$$m_r = \rho \cdot \eta_v \cdot n \cdot VD \tag{19}$$

The correlations of isentropic and volumetric efficiencies are obtained by curve-fitting the n-η_s and n-η_v chart presented by the manufacturer. These correlations have the following form:

Table 4
The coefficients of Isentropic and volumetric efficiencies equations (wobble plate type SD7H15 taken from SANDEN CO.).

Discharge pressure (Psig)	a1 b1	a2 b2	a3 b3	a4 b4
202	0.5720705e−9 0.4367589e−9	−0.32311e−5 −0.4231926e−5	−0.2379907100e−2 0.33878611348e−2	63.7064051000 72.1159834791
250	0.9747379e−9 0.1148391e−8	−0.6404448e−5 −0.9410138e−5	0.54470967060e−2 0.14663638218e−1	59.6576660131 62.0291796771
303	0.7468923e−9 0.6115190e−9	−0.4777637e−5 −0.5304138e−5	0.28887030711e−2 0.60665912440e−2	59.5738353238 62.8234128121
366	0.1029154e−8 0.5609421e−9	−0.7587007e−5 −0.5348830e−5	0.11960628030e−1 0.84594346518e−2	51.3203515175 54.9072135411

$$\eta_s = a_1 n^3 + a_2 n^2 + a_3 n + a_4 \tag{20}$$

$$\eta_v = b_1 n^3 + b_2 n^2 + b_3 n + b_4 \tag{21}$$

Table 5
Operating conditions of simulation.

Air temperature entering evaporator (T_{aie})[a]	27 [°C]
Air temperature entering condenser (T_{aic})[a]	35 [°C]
Volumetric flow rate of air streams in evaporator (V_{ae})	500 [$m^3\ h^{-1}$]
Degree of superheat (ΔT_{sh})	5 [°C]
Velocity of air streams in condenser (u_{ac})	4 m [s^{-1}]
Volumetric Displacement (VD)[b]	154.9 [cc°s^{-1}]
Rotational speed of compressor (n)[a]	1800 [rpm]

[a] JIS D1618-1986 (Japanese Industrial Standard, 1988).
[b] Technical datasheets of wobble plate type SD7H15 taken from SANDEN Co.

According to the data sheet, the considered compressor was taken from Sanden Co., the coefficients 'a' and 'b' are related to discharge pressure as mentioned in Table 4. For the different discharge pressures, an interpolation or extrapolation needs to be done.

4. Program flow chart and operating condition

The program codes of the thermodynamic cycle simulation were written in MATLAB, and for extracting the necessary thermodynamic properties in the program the REFPROP software was linked with MATLAB. The written program contains a main program and some sub-programs for the evaporator, compressor and condenser. The input parameters are according to Table 5.

The outputs are COP, the system cooling capacity, compressor power consumption, compressor discharge pressure, evaporator

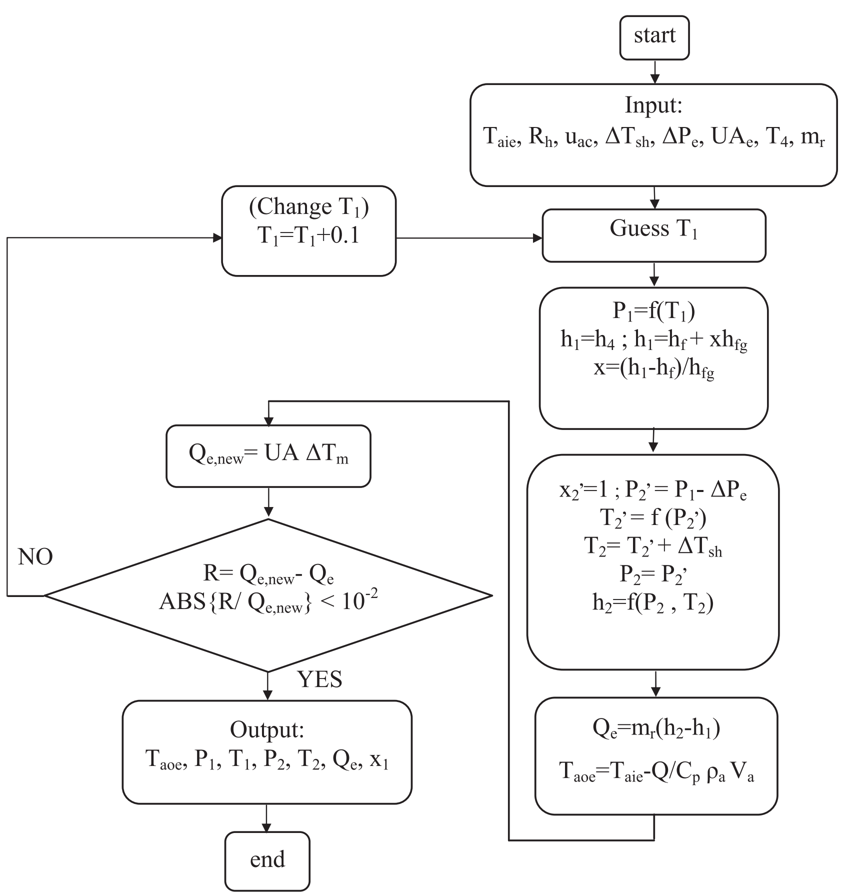

Fig. 4. Flow chart of performance analysis program for the evaporator.

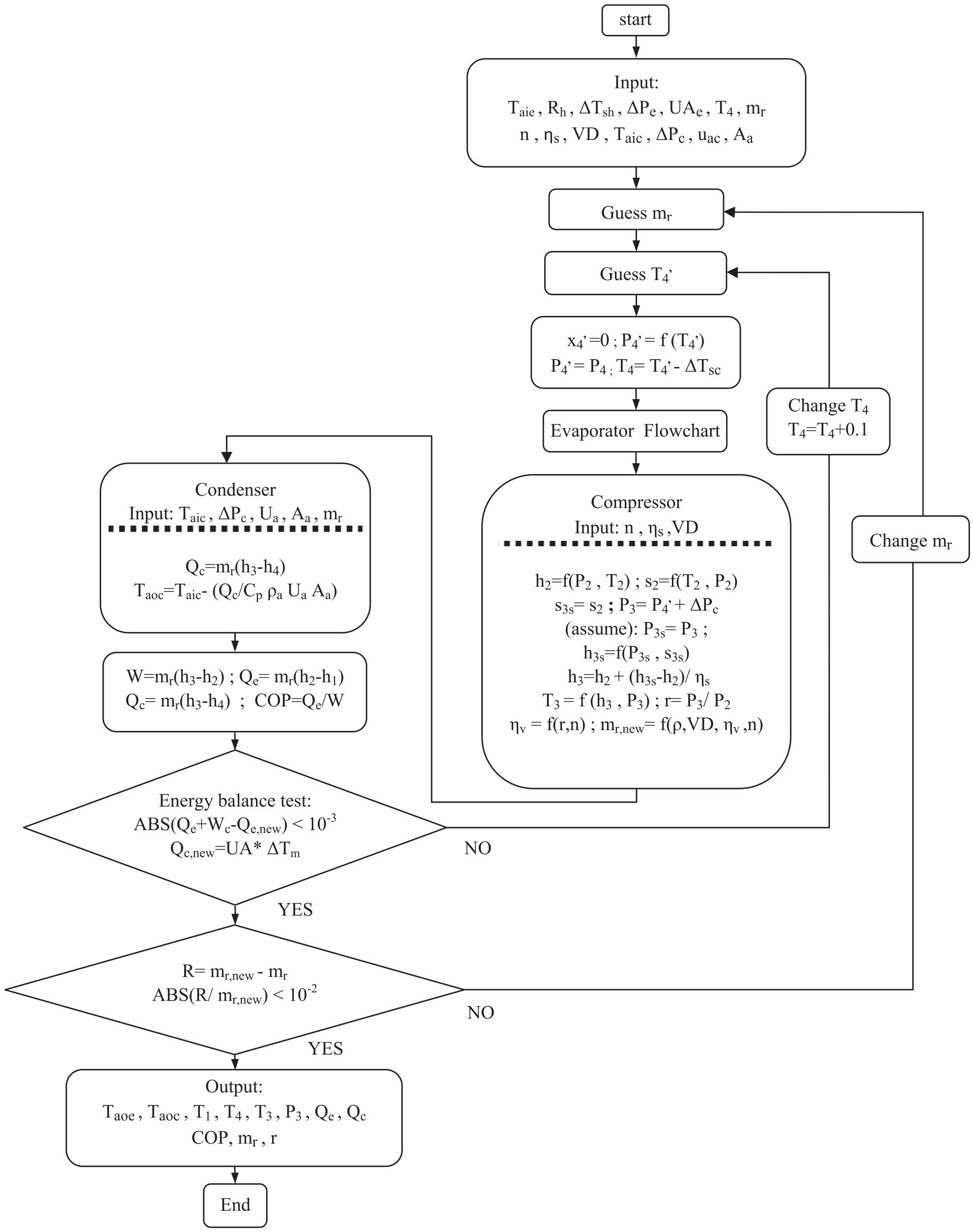

Fig. 5. Flow chart of performance analysis program for the main cycle.

and condenser outlet air temperature and pressure ratio. The program flow charts are shown in Figs. 4 and 5.

5. Results and discussions

On the assumed automotive A/C system, a comprehensive simulation was done. The system performance was investigated in two states: for the first state, the cooling capacity is taken constant at $Q_e = 3.5$ kW, and the refrigerant mass flow rate would be changeable. At the second state, the mass flow rate was considered constant at $m_r = 113\ \mathrm{kg\ h^{-1}}$ (which is taken from SANDEN Co. Qazvin branch). The performance analysis of the cycle with mini-channel heat exchangers is discussed and compared for HFO-1234yf and HFC-134a as the working fluids.

For the result adaptation by the on-road automotive condition it should be added that there is no absolutely constant mass flow rate or constant cooling capacity state. Cooling capacity may be variable by the interior of the automotive, and the amount of mass flow rate circulating the cycle is dependent on the speed of the compressor and changes with the rpm of the engine. In this study, we considered two mentioned states for a correct comparison between HFO-1234yf and HFC-134a. For this reason, the effect of outstanding interior and exterior parameters of automotive are investigated on the performance of the A/C. These operating parameters refer to the wind speed that impresses the air inlet velocity of the condenser (U_{aic}) and the ambient engine temperature, which both affect the condenser air inlet temperature (T_{aic}) and the temperature of the interior of the automotive that effects the air inlet temperature of the evaporator (T_{aie}).

Fig. 6 reports the heat transfer coefficients during condensation of HFO-1234yf and HFC-134a at 44 °C saturation temperature and a mass flux of 200 $\mathrm{kg/m^2\ s}$ over the entire range of vapor quality. The coefficient of heat transfer increases during the condensation,

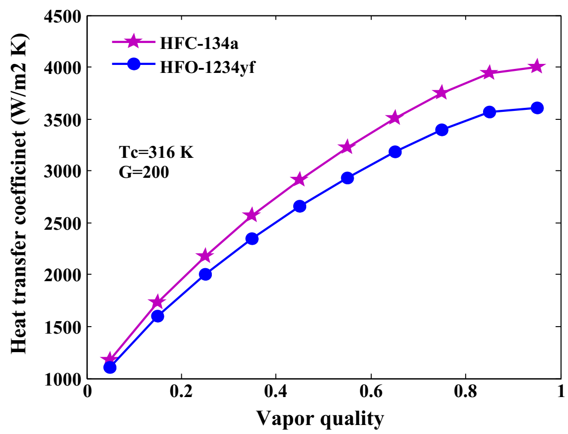

Fig. 6. Local heat transfer coefficient versus vapor quality with HFO-1234yf and HFC-134a during condensation.

and the vapor quality increases in the mini-channel heat exchanger. Also, it seems that the HFC-134a heat transfer coefficient is 6–9% higher than HFO-1234yf, which has agreement with the results of experimental work by Del et al. [21]. In their work, the local heat transfer coefficient was measured during condensation of HFO-1234yf and HFC-134a in a circular mini-channel [21]. At a 44 °C saturation temperature, HFO-1234yf has 20% lower liquid thermal conductivity, which affects the thermal resistance of the liquid film. Therefore, the mean heat transfer coefficient of condensation of HFO-1234yf would be lower.

Fig. 7 shows the variation of the overall heat transfer coefficient with condenser inlet air velocity and refrigerant mass flux varying between 200 and 550 kg/m2 s for T_c = 44 °C. The UA increases by increasing the inlet air velocity and the refrigerant mass flux. Thus, UA can be represented as a function of inlet air velocity and refrigerant mass flux. By considering the effect of mass flux at equal air velocity, it is found that the overall heat transfer coefficient grew when the mass flux rose. This is due to increasing the convective heat transfer by increasing the vapor velocity, which occurs by raising heat flux. As a result, the overall heat transfer coefficient is increased. Also, it is observed that overall heat transfer coefficient of HFO-1234yf is lower than that of HFC-134a by about 18–21% in the same operating conditions and this is because of the different properties of the two refrigerants.

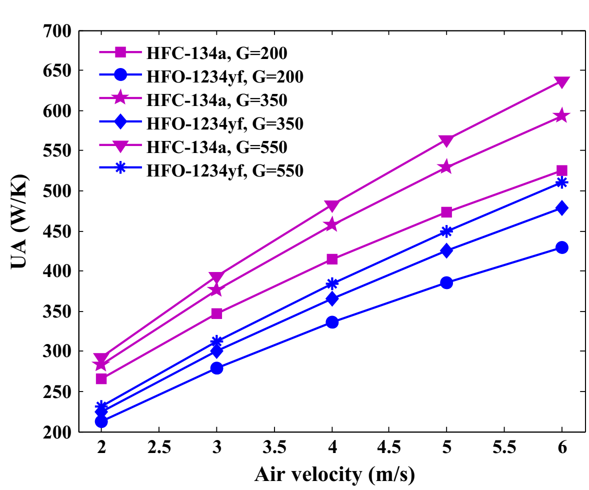

Fig. 7. Variation of the refrigerant-side overall heat transfer coefficient with inlet air velocity of condenser and refrigerant mass flow rate.

The effect of refrigerant mass flux on refrigerant-side pressure drop during condensation and evaporation of HFC-134a and HFO-1234yf is shown in Fig. 8 at both 0 °C and 44 °C saturation temperatures of evaporating and condensing, respectively. It is observed that the refrigerant-side pressure drop increases by increasing mass flux in the evaporation and condensation processes. The enhancement of mass flux will raise the vapor velocity; thereafter, the pressure drop would increase. It is found that HFO-1234yf performs better than HFC-134a due to the lower value of average pressure drop of HFO-1234yf (24% during condensation and 20% during evaporation).

Fig. 9 shows the variation of the air-side pressure drop and heat transfer coefficient with inlet air velocity of the condenser, where the air temperature is considered constant at 35 °C. From this figure, it seems that the heat transfer coefficient and the pressure drop increase with increasing air velocity. The obtaining results shown on the curves demonstrate that the effect of air velocity is significant on pressure drop. The performances of refrigerants containing HFO-1234yf and HFC-134a are calculated, and the results are shown in Table 6.

According to the results, the obtained COP is at a maximum point for HFO-1234yf. The lower the T_{dis} and pressure ratio allocated to HFO-1234yf, the less the amount of T_{dis} and pressure ratio raise COP and increase compressor durability. The experimental

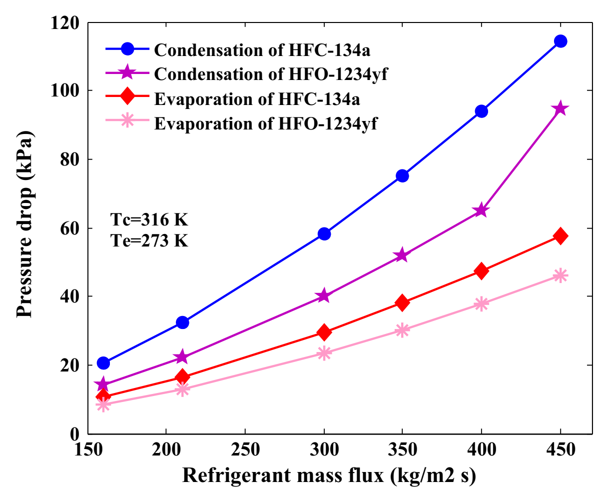

Fig. 8. Effect of refrigerant mass flux on refrigerant-side pressure drop during condensation and evaporation of HFC-134a and HFO-1234yf.

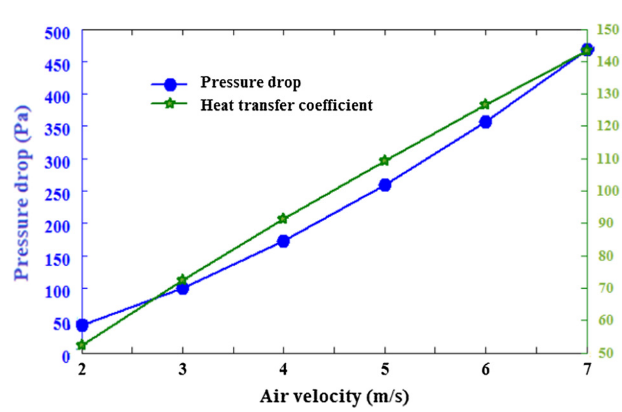

Fig. 9. Variation of the air-side heat transfer coefficient and pressure drop with inlet air velocity.

Table 6
Comparison of system performance with HFC-134a and HFO-1234yf.

Refrigerant	COP	Q_e (kW)	W_{comp} (kW)	T_{dis} (°C)	P_{dis} (kP)	r	T_1 (°C)	T_4 (°C)	P_1 (kPa)
HFC-134a	2.07	4.20	2.03	82.0	1208.6	6.1	−5.4	44.2	237.42
HFO-1234yf	2.45	3.34	1.36	61.9	1165.9	4.2	0.5	42.8	318.50

results have agreement with this statement and the compressor T_{dis} of HFO-1234yf is 5–9% lower than of HFC-134a [22]. Looking at the first state, different parameters including fluid mass flow rate, compressor work, condenser heat rejection and COP are reported in Figs. 10–13 for both refrigerants.

According to Fig. 10, the mass flow rate of HFO-1234yf is higher than of HFC-134a. For justification, we can refer to the T-h diagram where the vaporization enthalpy of HFO-1234yf is lower than HFC-134a. Therefore, for the equal cooling capacity, the mass flow rate of HFO must be higher. The HFO-1234yf average mass flow rate is 27% higher than HFC-134a, which may be validated by other work [21] wherein that difference has been reported at 23–35%. As depicted in Fig. 11, HFO-1234yf has higher condenser heat rejection; the main reason for this is in the results of Fig. 10, where HFO-1234yf has a higher mass flow rate than HFC134a, and this causes more heat transfer in the condenser and one can design a smaller condenser in optimization.

According to Fig. 12, the compressor work for compressing HFC-134a is slightly higher than for HFO-1234yf when considering the constant evaporator cooling capacity, and this higher level of work makes for a slightly lower COP level for HFO-1234yf according to Fig. 13. The COP of HFO-1234yf with changing compressor rpm is 1.3–5% lower than HFC-134a, which is in good agreement with the previous work [10] that reported 0–4% lower COP. The conformity of the simulated model for HFC-134a was also checked by Kayanakli and Horuz [23] (Fig. 14).

The system performance was investigated in the second state as well (Figs. 15–19). Where the conditions were simulated with what happens in the realistic comparative situations and in a constant mass flow rate state, the performance of two refrigerants was compared. Increasing condenser inlet air velocity results in a decrease in the condensing pressure, therefore leading to a lower compressor power and a higher cooling capacity, and these phenomena make higher COPs (Figs. 15 and 16).

According to Fig. 15, at the lower levels of condenser air velocity, increasing a small amount of air velocity causes a large increase on the heat rejection because the evaporator surface is cool and it has a capacity for cooling the air. But considering a high amount of air velocity (5–7 m/s), it doesn't have any significant effect on the

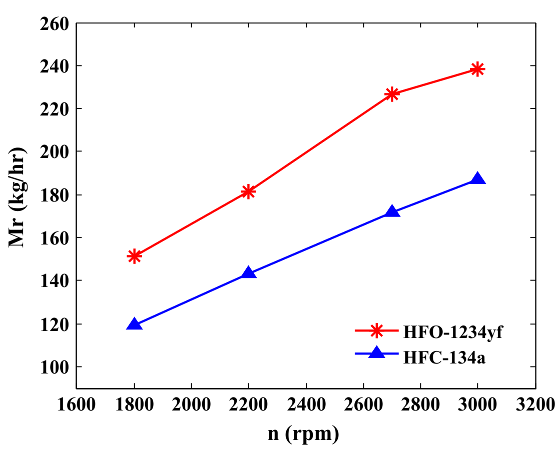

Fig. 10. Effect of n (rpm) on refrigerant mass flow rate at constant cooling capacity.

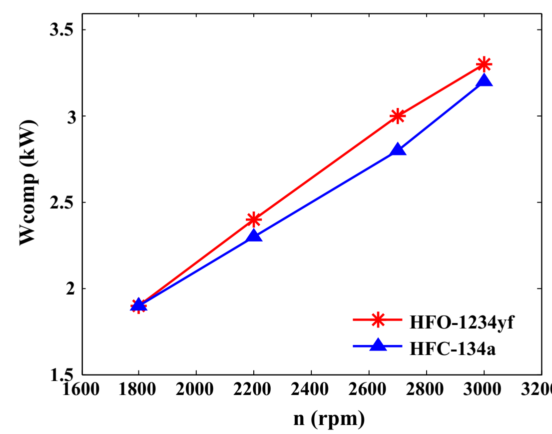

Fig. 12. Effect of n (rpm) on compressor work at constant cooling capacity.

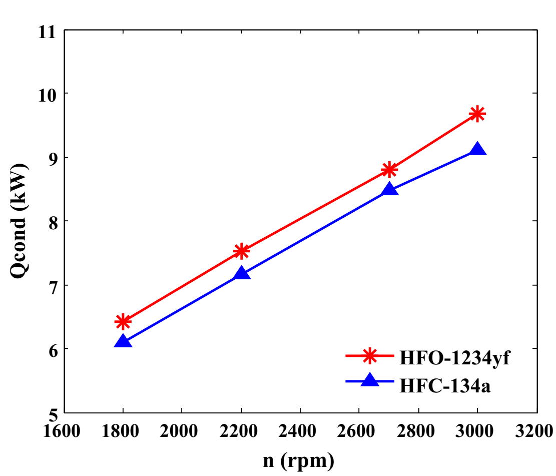

Fig. 11. Effect of n (rpm) on condenser heat rejection at constant cooling capacity.

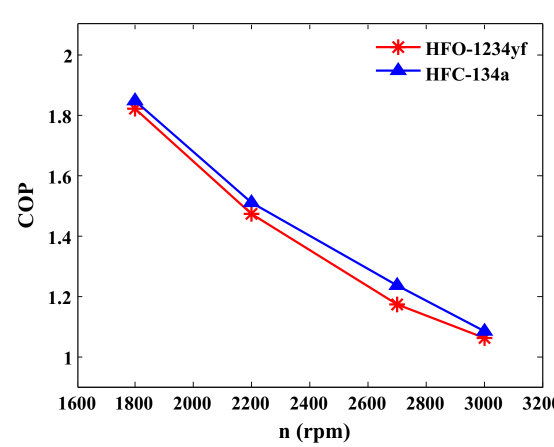

Fig. 13. Effect of n (rpm) on system COP at constant cooling capacity.

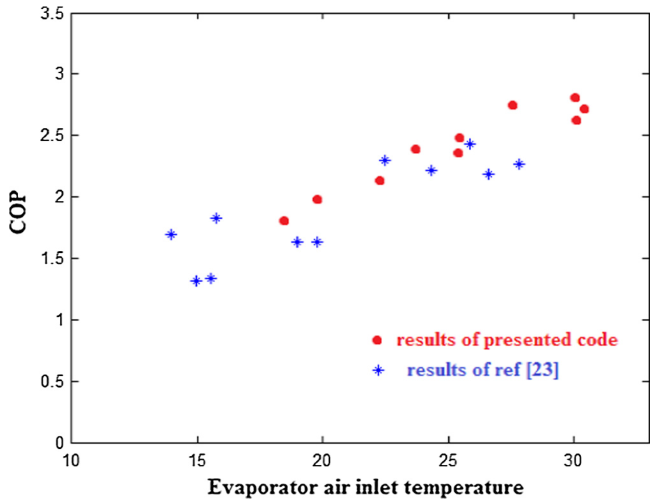

Fig. 14. Validation of the performance results.

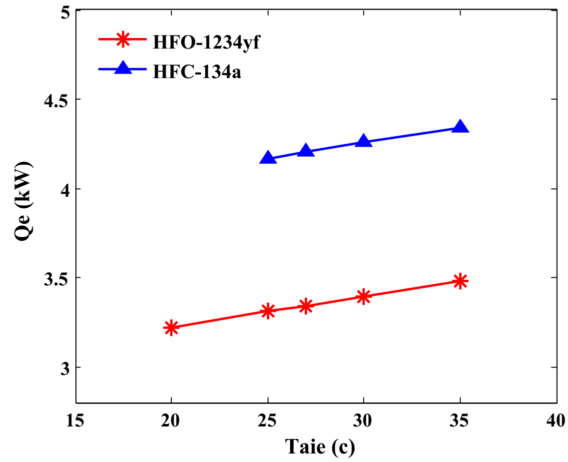

Fig. 17. Effect of T_{aie} on cooling capacity at constant refrigerant mass flow rate.

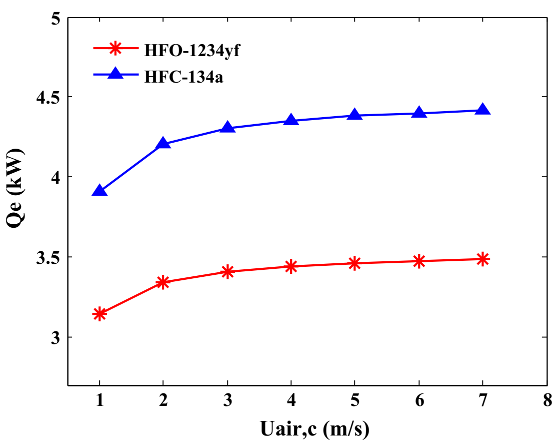

Fig. 15. Effect of condenser inlet air velocity on cooling capacity at constant refrigerant mass flow rate.

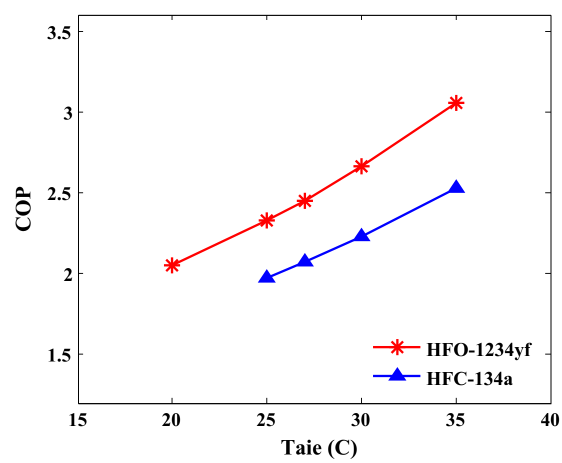

Fig. 18. Effect of T_{aie} on system COP at constant refrigerant mass flow rate.

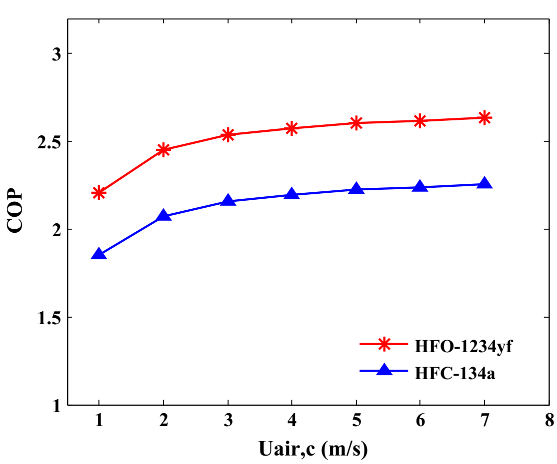

Fig. 16. Effect of condenser inlet air velocity on system COP at constant refrigerant mass flow rate.

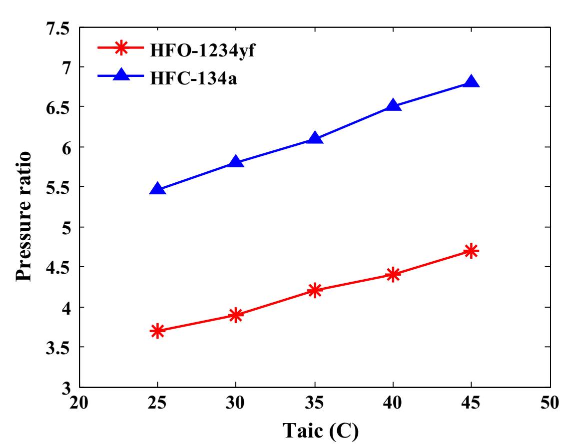

Fig. 19. Effect of T_{aic} on pressure ratio at constant refrigerant mass flow rate.

cooling capacity because it has reached so-called cooling saturation states. Also, with increasing evaporator inlet air temperature, Q_e, COP would consequently increase. It's clear that the higher air inlet temperature leads to the larger heat transfer with the cold body (evaporator) (Figs. 17 and 18). These results conform to the results of [23].

The effect of increasing condenser inlet air temperature on pressure ratio is shown in Fig. 19. The COP changes versus condenser inlet air temperature (T_{aic}) are descending according to

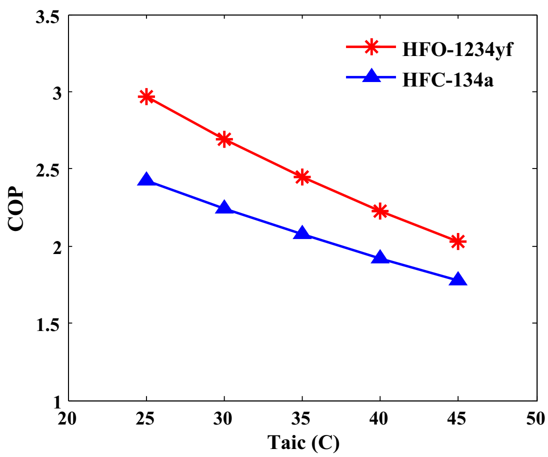

Fig. 20. Effect of condenser inlet air temperature on COP at constant refrigerant mass flow rate.

Fig. 20. Increasing T_{aic} causes decreasing heat transfer in the condenser, so COP drop would happen.

The decreasing pressure ratio is directly effective on increasing COP, and HFO-1234yf possesses the lower pressure ratio at all ranges of T_{aic}. According to this figure and considering the standard operating condition, when T_{aic} is 35 °C, the COP of HFO-1234yf becomes 18% higher than of HFC-134a.

6. Conclusion

The theoretical work has been performed to simulate the automotive air conditioning by considering HFO-1234yf as a drop-in replacement of HFC-134a. The model simulated in this paper predicted the experimental data with appropriate accuracy. The following conclusions are made:

- The refrigerant-side overall heat transfer coefficient of HFO-1234yf is 18–21% lower than that of HFC-134a in the mini-channel heat exchanger in the same operating conditions.
- As the pressure drop of HFO-1234yf is smaller during condensation and evaporation, HFO-1234yf performs better than HFC-134a.
- The discharge temperature of compressor and pressure ratio of HFO-1234yf is lower than HFC-134a, which can increase the compressor durability.
- The working pressure of HFO-1234yf is lower than that of HFC-134a, which may be effective for increasing COP. Having lower working pressure results in using a piping system with less thickness, lower price and higher proficiency.
- In the constant mass flow rate state, the COP of HFO-1234yf is 18% higher than that of HFC-134a.
- In a constant cooling capacity, the mass flow rate of HFO-1234yf is 27% higher than that of HFC-134a.
- In identical cooling capacity, the COP of HFO-1234yf is 1.3–5% lower than that of HFC-134a.

Acknowledgement

The sixth author would like to thank the “Research Chair Grant” National Science and Technology Development Agency (NSTDA), the Thailand Research Fund (TRF) and the National Research University Project (NRU) for the support.

References

[1] J.S. Brown, C. Zilio, A. Cavallini, Thermodynamic properties of eight fluorinated olefins, Int. J. Refrig. 33 (2) (2010) 235–241.
[2] J.S. Brown, S.F. Yana-Motta, P.A. Domanski, Comparitive analysis of an automotive air conditioning systems operating with CO_2 and R134a, Int. J. Refrig. 25 (1) (2002) 19–32.
[3] K.A. Joudi, A.S.K. Mohammed, M.K. Aljanabi, Experimental and computer performance study of an automotive air conditioning system with alternative refrigerants, Energy Convers. Manage. 44 (18) (2003) 2959–2976.
[4] S. Wongwises, A. Kamboon, B. Orachon, Experimental investigation of hydrocarbon mixtures to replace HFC-134a in an automotive air conditioning system, Energy Convers. Manage. 47 (11) (2006) 1644–1659.
[5] K. Mani, V. Selladurai, Experimental analysis of a new refrigerant mixture as drop-in replacement for CFC12 and HFC134a, Int. J. Therm. Sci. 47 (11) (2008) 1490–1495.
[6] E. Arcaklıoğlu, A. Çavuşoğlu, A. Erişen, Thermodynamic analysis of refrigerant mixtures for possible replacements for CFCs by an algorithm compiling property data, Appl. Therm. Eng. 26 (4) (2006) 430–439.
[7] M. Spatz, B. Minor, HFO-1234yf low GWP refrigerant update-Honeywell & Dupont joint collaboration, in: International Refrigerant & Air Conditioning Conference, Purdue, July, 2008.
[8] O. Nielsen et al., Atmospheric chemistry of CF_3CFCH_2: kinetics and mechanisms of gas-phase reactions with Cl atoms, OH radicals, and O_3, Chem. Phys. Lett. 439 (1) (2007) 18–22.
[9] J.S. Brown, C. Zilio, A. Cavallini, The fluorinated olefin R-1234ze (Z) as a high-temperature heat pumping refrigerant, Int. J. Refrig. 32 (6) (2009) 1412–1422.
[10] C. Zilio, J.S. Brown, A. Cavallini. Simulation of R-1234yf performance in a typical automotive system, in: Proceedings of the 3rd Conference on Thermophysical Properties and Transfer Processes of Refrigeration, Boulder, CO, USA, Paper, 2009.
[11] S. Zhang, H. Wang, T. Guo, Evaluation of non-azeotropic mixtures containing HFOs as potential refrigerants in refrigeration and high-temperature heat pump systems, Sci. China Technol. Sci. 53 (7) (2010) 1855–1861.
[12] G.D. Mathur, Experimental performance of a parallel flow condenser with HFO-1234yf as the working fluid, 2010 (SAE Technical Paper).
[13] Y. Lee, D. Jung, A brief performance comparison of R1234yf and R134a in a bench tester for automobile applications, Appl. Therm. Eng. 35 (2012) 240–242.
[14] J. Navarro-Esbrí et al., Experimental analysis of R1234yf as a drop-in replacement for R134a in a vapor compression system, Int. J. Refrig. 36 (3) (2013) 870–880.
[15] A. Mota-Babiloni et al., Drop-in energy performance evaluation of R1234yf and R1234ze (E) in a vapor compression system as R134a replacements, Appl. Therm. Eng. 71 (1) (2014) 259–265.
[16] Z. Janković, J.S. Atienza, J.A.M. Suárez, Thermodynamic and heat transfer analyses for R1234yf and R1234ze (E) as drop-in replacements for R134a in a small power refrigerating system, Appl. Therm. Eng. 80 (2015) 42–54.
[17] J. Dong et al., Heat transfer and pressure drop correlations for the multi-louvered fin compact heat exchangers, Energy Convers. Manage. 48 (5) (2007) 1506–1515.
[18] W. Li, X. Wang, Heat transfer and pressure drop correlations for compact heat exchangers with multi-region louver fins, Int. J. Heat Mass Transf. 53 (15) (2010) 2955–2962.
[19] M.-H. Kim, C.W. Bullard, Development of a microchannel evaporator model for a CO_2 air-conditioning system, Energy 26 (10) (2001) 931–948.
[20] G. Lee, J. Yoo, Performance analysis and simulation of automobile air conditioning system, Int. J. Refrig. 23 (3) (2000) 243–254.
[21] D. Del Col, D. Torresin, A. Cavallini, Heat transfer and pressure drop during condensation of the low GWP refrigerant R1234yf, Int. J. Refrig. 33 (7) (2010) 1307–1318.
[22] G.D. Mathur, Experimental investigation of AC system performance with HFO-1234yf as the working fluid, 2010 (SAE Technical Paper).
[23] Ö. Kaynaklı, I. Horuz, An experimental analysis of automotive air conditioning system, Int. Commun. Heat Mass Transf. 30 (2) (2003) 273–284.